

A Polarizable Force Fields for Bio-compatible Ionic Liquids Based on Amino Acids Anions.

Stefano Russo^a and Enrico Bodo^{a*}

^aDepartment of Chemistry, University of Rome “La Sapienza”, Rome, Italy;

*Corr. Author: Enrico Bodo, Department of Chemistry, University of Rome “La Sapienza”, Piazzale Aldo Moro 5, 00185, Rome. Email: enrico.bodo@uniroma1.it

A Polarizable Force Fields for Bio-compatible Ionic Liquids Based on Amino Acids Anions.

We present a polarizable force field parametrization for amino acid-based ionic liquids based on the Amoeba framework. The force field has been obtained using accurate ab-initio data and has been conceived to be as compatible as possible with the existing Amoeba parametrization. We present here a validation mainly carried out using reference ab-initio calculations and we show how the parametrization is able to provide the structural features of the fluids to an excellent extent as well as to reproduce the intermolecular interaction energies.

Keywords: force fields; molecular dynamics; ionic liquids, amino acids

1. Introduction

Biocompatible ionic liquids, despite being made by simple molecular ions such as deprotonated amino acids (AA), show a surprisingly complex dynamics and a range of phenomena that challenge the traditional way of approaching their computational simulations, especially if we desire to study them in increasingly complex setups that emerge in the new technologies of societal relevance like new generation batteries, sustainable bio-materials, nanomedicine. [1–6]

Ionic Liquids (ILs) have represented, in the past few decades a significant opportunity to replace some of the more harmful organic solvents currently used in various fields such as dissolution of biomasses [7], electrochemistry [8,9], corrosion inhibition [10], catalysis [11], and polluting gases removal [12–17]. For a long time, their extremely low volatility and high chemical stability made them inherently “greener” replacements for traditional, often environmentally harmful, chemical solvents. A more recent set of studies targeted at quantifying their biocompatibility has discovered that many ILs are often toxic and less environmentally-benign than previously assumed [18–

20]. Despite this experimental evidence, a fundamental understanding of their action toward biomolecules at the molecular level has only been seldom explored [21–23].

Fully biocompatible ILs represent a most recent incarnation of these substances and are typically made using the choline cation as a replacement of imidazolium [1,2,6] and a deprotonated AA anion (AA based ILs, AAILs). AAILs pertain to the class of ILs known as protic ILs where ionization occurs because of a (formal) proton exchange reaction where the AA is the proton donor. The proton exchange reaction leads to the appearance of an extensive and intricated network of hydrogen bonds (HBs) that is the source of their gentle solvation properties. Such ability has, in turn, spawned a concrete interest for the use of these substances in medicine [4,24], circular economy [25–27] and electrochemistry [8,28,29]. If the use of biocompatible ILs should become as pervasive as the current interest induces to expect, a proper modelling of their toxicity, biocompatibility, biodegradability will be mandatory soon. While evidence from in-vivo experiments is already available [30,31], simulations about this subject are still scarce and in an early stage [31–33].

Simulations of the bulk state of ILs are typically performed using Molecular Dynamics (MD) [34,35] where a simplified representation of the molecular systems is employed. The complexity of the nuclear and electronic quantum time evolution is blended into a topologically bound set of atoms or other entities whose quantum properties are neglected, and the interatomic/intermolecular forces are computed from a simple and computationally efficient parametrization that is named the “force field” (FF). The reliability of the results obtained from the simulations depends entirely on the quality of the FF.

In order to extend the studies of these substances from the pure bulk phase [36–39] to their interaction with bio-molecules (even if only at the level of test case studies)

a reliable FF and an efficient computational model is needed. In this context, it has long been recognized that, in order to be able to reproduce correctly the dynamic inside the fluid [40,41], hence solvation, the FF has to take into account polarization and possibly charge transfer effects. [42–47] This is the purpose of “polarizable” FFs [48,49]. Polarizable FFs typically ensure a more realistic description of dynamical quantities such as fluidity, ionic mobility, and conductivities, all of which are underestimated by non-polarizable models [42]. For the study of AAILs, polarization is crucial: an accurate representation of the HBs network (essentially electrostatic in origin) is mandatory to properly determine the structure and the dynamics of the fluid within the solvation shell of biomolecules.

The current status of parametric FFs for ionic liquids have been recently summarized in refs. [50,51]. In non-polarizable FFs, the partial atomic charges are fixed, and electrostatic interactions are computed from a sum of two body (typically atom-atom) interactions. In the real ionic systems, the partial atomic charges fluctuate depending on the chemical surrounding because of induction effects. In polarizable FFs, the two-body sum is modified to account for these effects, including induction energies and the many-body electrostatic interaction arising from them (e.g., dipole-dipole and charge-induced dipole).

A part of the community is already involved in the study and realization of polarizable FFs. We mention the recent availability of the CL&Pol [49,52,53] and Amoeba-IL [48] FFs. Both aims at becoming a sort of “standard” for polarizable simulations of ILs, but neither of them at the moment include a parametrization for AAILs.

In this paper we present a parametrization of a polarizable FF for AAILs that relies on the Amoeba model. The FF derivation is based on a physical approach to electrostatic

induction and does not use additional particles (core shell models) to account for it. The drawback is that the Amoeba polarization model requires a specifically tailored algorithm to calculate the electrostatic energy. The additional computational cost of this algorithm is overcome by the recent development of a highly parallel version of the Tinker software (Tinker-HP) that has been recently proven very effective [54].

The choice of working within the Amoeba model, has been motivated by the fact that it already encompasses a well-tested parametrization for biomolecules. Providing a fully compatible FF with the already existing parametrization should provide a simple way of moving toward the study of biomolecules solvation in AAILs.

2. Parametrization

The Amoeba FF potential energy is reported in refs. [48,55,56]. The energy is divided into a topologically bound, short range component and a long range one. The former consists in a fourth and sixth order expansion of bond and angle energies respectively, plus additional terms for torsional energy and out-of-plane bending. Several coupling terms are also introduced. The long-range components are the Van der Waals one (calculated through a pairwise, atom-atom sum of “buffered 14-7” potential forms) and electrostatic. The main difference of Amoeba with respect to other FFs lies in the way the electrostatic term is built. This interaction is calculated using an atom-centred expansion on permanent monopoles, dipoles and quadrupoles plus the polarization and induction energies generated by allowing the existence of a non-permanent dipole on each atom induced by the surrounding charge distribution. The Thole model of smeared electronic charges is employed to avoid the so-called polarization catastrophe. [57]

In order to provide the entire set of parameters needed by Amoeba to compute the potential energy of a given molecule, one generally extracts the parameters from high-quality ab-initio calculations on isolated molecules. Of great help in performing the

complicated sequence of computations is the poltype tool [58] which has been purposely written to ease this task.

Within the poltype procedure, following a recent assessment of the performance of functionals and basis sets combinations in describing ionic liquids [59], the optimization of the molecular ions has been done using the ω B97X-D3 functional and the 6-31G* basis set. The electric multipoles have been determined using MP2/6-311G**. The atomic charges have been fitted using the interpolation of the electrostatic field as generated by the electronic density at the MP2/6-311++G(2d,2p) level.

This technique has been applied to the calculation of the amoeba FF parameters of 9 AA anions ([Ala], [Gly], [Cys], [Ser], [Val], [Asp], [Lys], [His] and [Phe]) and of the cholinium cation ([Ch]). All parameters are available as single files in the tinker format as supporting material. [60] An assessment of the quality of the determination of the short range topologically bound FF parameters and of the electrostatic fitting for the 10 isolated ions (RMSD between the ab-initio and FF minimum geometry and on the fitting of the ion-generated electric potential) are reported in Table S1.

Each ion has been treated as an isolated molecule with an overall integer charge (obviously $\pm 1e$). Setting an integer charge on each ion is mandatory to obtain a transferable FF, but this also means that we cannot fully consider charge transfer phenomena. The latter consists in the fact that, in the bulk phase, the molecular ions of an IL do not appear to retain the integer charge, but rather a reduced one which can be significantly lower than 1 in absolute value [41,61]. It is important to remark this drawback of our approach because, due to the lack of certain experimental data in the literature, we have not been able to validate the present FF against ionic mobility properties and an additional scaling of the ionic charges [41] might be necessary in certain given applications (calculating diffusivity for example).

Another issue that can arise in the modelling of AAILs is related to proton transfer. Within a fixed chemical topology model (such as the one presented here), this effect cannot be considered. For most of the AA anions this is not a problem because they do not have any mobile proton on their chemical structure (the carboxylic proton has already been lost), but some of them can have an additional proton on the side chain. These are, for example, the [Cys], [Lys] and the [Asp] anions. The deprotonation of the side chain of [Cys] and [Lys] appears extremely unlikely [62], but for [Asp] could be more efficient (leading eventually to the formation of zwitterionic structures). We point out that the present parametrization cannot take into account this effect.

3. Validation

As a starting point we checked the ability of our FF to reproduce the ionic couple interaction energies comparing it to literature data and to purposely computed values. We have also extended such validation to larger clusters made by an increasing number of ionic couples up to five to verify the ability of the present FF in reproducing the build-up of many-body energies. As the reference ab-initio calculations, we have specifically employed the ω B97X-D3 [59,63,64] functional coupled with either a cc-pVTZ basis on the isolated ionic couples, and the smaller cc-pVDZ on the clusters with more ionic couples.

To assess the quality of our FF in describing the bulk phase, constant pressure simulations have been used to calculate the “natural” densities achieved by the FF parametrization and compared to the available experimental data. Finally, the structure of the bulk fluid stemming from our FF has also been validated using our previous data obtained using ab-initio MD (e.g. see [37]) and through the calculation and comparison of X-ray structure factors.

3.1 Interaction energies in ionic couples and clusters

The interaction energies of the 9 ionic couples [Ch][AA] as computed using the reference DFT method and the FF are reported in Table 1 (and as a bar plot in Figure S8). Each ionic couple has been optimized at its minimum geometry using the previously indicated methods. The interaction energy has been then computed as the difference between the electronic energy of the two optimized ionic fragments and the ionic couple. The performances of the FF are measured by a percentage error that is well below 10% for most AA and peaks at 8% and 7% for [Gly] and [Asp]. Overall, this is an indication of a very decent performance of the FF to reproduce the anion-cation interaction. We point out that the interaction energies computed using a functional without the dispersion interactions (B3LYP) as taken from ref. [65] are systematically lower than both the dispersion corrected ω B97X-D3 and the FF results.

Table 1: Interaction energies of the [Ch][AA] ionic couples in kcal/mol. The %Error is calculated with respect to the ω B97X-D3/cc-pVTZ ab-initio value. The geometric RMSD has been calculated by first realigning both structures.

[AA] anion	Present FF kcal/mol	ω B97X-D3 kcal/mol	%Error	RMSD (Å)	B3LYP ^a kcal/mol
[Ala]	108.94	115.25	5.47	0.53	107.7
[Cys]	106.11	105.59	0.48	0.89	106.3
[Gly]	111.14	121.69	8.67	0.68	103.5
[Ser]	105.95	109.47	3.22	0.50	106.9
[Val]	109.46	112.35	2.57	0.80	106.3
[Asp]	115.37	124.26	7.16	0.31	104.9
[Lys]	115.39	117.88	2.11	0.37	105.8
[Hys]	113.17	116.95	3.23	0.36	102.7
[Phe]	106.41	113.96	6.62	0.18	104.3

^a The values in the B3LYP column are taken from ref. [65]

The geometry of each ionic couple is perfectly reproduced by the force field when compared to the reference geometry emerging from DFT. The RMSD detected for each ionic couple are only slightly larger than those of the single ions (Table S1), as expected, but still lie well within 1 Å and many do not exceed 0.5 Å. A pictorial example of the

geometric agreement is provided in Figure 1 where we report the best ([Ch][Phe]) and worst ([Ch][Cys]) cases.

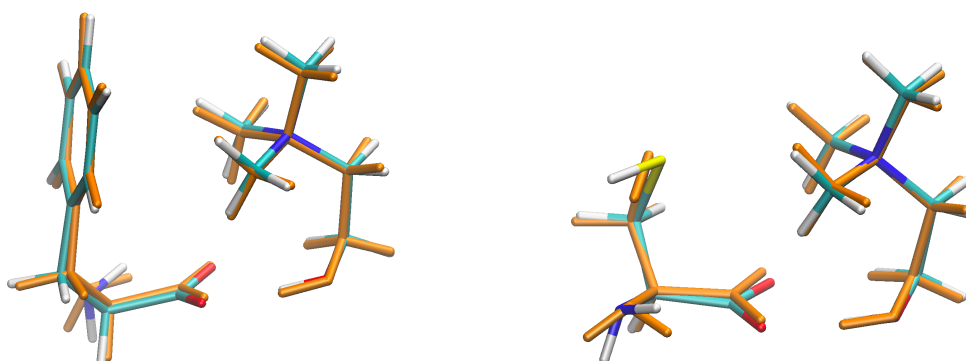


Figure 1: Ionic couple minimum geometry within our Amoeba model (colors) and from DFT reference calculations (orange). Left, [Ch][Phe]; right, [Ch][Cys].

The issues bound to interionic charge transfer, mentioned in the parametrization section, can be readily quantified here by calculating the net ionic charge carried by each ion using the ω B97X-D3 electron density. The evaluation of the NBO charges on the ionic couples reveals that the net ionic charge ranges between 0.86 and 0.89 with very little variation along the AA series. This sizable tendency of the ions to lose part of their charge represents an inevitable possible source of inaccuracies in evaluating with the FF both energetic and frictional properties of the bulk phases.

The performance of the FF in describing larger ionic aggregates has been measured by applying the above method to clusters made by 2, 3, 4 and 5 ionic couples. The procedure we have used to obtain the energies is the following: (i) we have run a short MD of the isolated cluster at high temperature in order to generate a disordered geometry; (ii) we have optimized this geometry using our Amoeba FF; (iii) the resulting structure was then reoptimized using DFT. This procedure allows us to compare the binding energy of the local minimum obtained with the FF with that stemming from DFT (arguably more accurate). Given the substantial computational cost of these computations, the procedure

has been only applied to 5 representative AA anions. The results are reported in Table 2. The FF, as in the ionic couples, tends to slightly underestimate the interaction energy with respect to the reference value from DFT. This behavior is consistent along all AA anions, except for [Cys] where the difference is negative and small. The ability of the FF to reproduce the geometries is however evident from the low values of the geometric RMSD which indicate a remarkable agreement of Amoeba geometries with the reference ones and how the minima of the FF and of DFT turn out to be very similar.

The error in the interaction energy of the cluster is due to two key factors: first, as we pointed out above, our model does not take into account the electronic delocalization between the ions and is unable to reproduce the aforementioned charge transfer effects that might contribute negatively to the overall interaction energy especially at a relaxed geometry. Secondly, the multipolar expansion of the electrostatic energy in Amoeba is still only an approximation to the real energy and the negative contribution of many-body terms to the interaction energy is naturally underestimated by the FF. In addition, we cannot exclude that the reported DFT values might also be affected by a non-negligible BSSE error (due to the double zeta basis set) hence appearing artificially slightly too negative. Overall, the present FF, is able to reproduce with great accuracy the geometric structure of large interacting systems and to provide interaction energies that differs by less than 10% of the reference DFT values.

Additional refining and tuning of the short range Van der Waals coefficients could improve the agreement of the interaction energy, but this route would face a major drawback: the FF has been conceived to be as compatible as possible with the already present Amoeba parametrization (e.g. its bio-molecule variant Amoeba-bio) and such refinement would inevitably depend on the choice of the DFT reference data, thus rendering the FF parameters peculiar with respect to this choice.

Table 2: Interaction energies of cluster of ionic couples in kcal/mol. The %Error is calculated with respect to the ω B97X-D3/cc-pVDZ ab-initio value. The geometric RMSD has been calculated by first realigning both structures.

Cluster	Present FF kcal/mol	ωB97X-D3 kcal/mol	%Error	RMSD (Å)
[Ch] ₂ [Ala] ₂	235.28	258.85	9.10	0.60
[Ch] ₃ [Ala] ₃	369.34	409.62	9.83	0.42
[Ch] ₄ [Ala] ₄	506.82	556.23	8.88	1.03
[Ch] ₅ [Ala] ₅	650.52	706.80	7.96	0.59
[Ch] ₂ [Cys] ₂	241.15	232.73	-3.49	0.32
[Ch] ₃ [Cys] ₃	373.35	358.02	-4.11	0.50
[Ch] ₄ [Cys] ₄	485.16	497.43	2.47	0.94
[Ch] ₅ [Cys] ₅	629.10	636.76	1.20	0.74
[Ch] ₂ [Gly] ₂	244.88	275.21	11.02	0.90
[Ch] ₃ [Gly] ₃	372.67	419.89	11.24	0.64
[Ch] ₄ [Gly] ₄	511.39	578.83	11.65	0.80
[Ch] ₅ [Gly] ₅	645.01	726.41	11.21	0.95
[Ch] ₂ [Ser] ₂	238.04	246.26	3.34	0.22
[Ch] ₃ [Ser] ₃	362.32	379.79	4.60	0.27
[Ch] ₄ [Ser] ₄	500.31	531.12	5.80	0.31
[Ch] ₅ [Ser] ₅	624.21	666.81	6.39	0.32
[Ch] ₂ [Val] ₂	235.71	255.89	7.88	0.80
[Ch] ₃ [Val] ₃	378.50	400.07	5.39	2.08

A clearer representation of the accuracy of the FF in reproducing interaction energies can be had by plotting the energy profiles of the interaction energy along the ionic couple dissociation against the reference DFT data. In this case, the results have been obtained using a scan over a given distance that, starting from the initial minimum, leads gradually to the ionic couple separation. The procedure is similar to what has been done in ref. [49], and the two molecular ions have been gradually displaced rigidly. In order to decompose the DFT energy we have used the SAPT [66] procedure as implemented in the Psi4 code [67].

A sample of our tests is reported in Figure 2 and Figure 3 for [Ch][Cys] and [Ch][Val] respectively, where we compare the total interaction energy, the electrostatic, and Van der Waals contributions as they emerge from the SAPT analysis of DFT data with those

coming from the FF. Additional examples for [Ser], [Gly] and [Ala] are reported in the SI in Figures S1-S3.

The agreement between the two sets of data is remarkable, except for a slightly overestimation of the repulsive energy at short range which arises because the electrostatic energy is less attractive in the FF when compared to the one emerging from SAPT (orange lines). The repulsive effect due to Van der Waals is perfectly reproduced (green lines). It is worth remarking that the geometries in these examples are not arising from optimizations, but the molecules are displaced rigidly thus avoiding preferred regions of the conformational space which could lead to a spurious agreement.

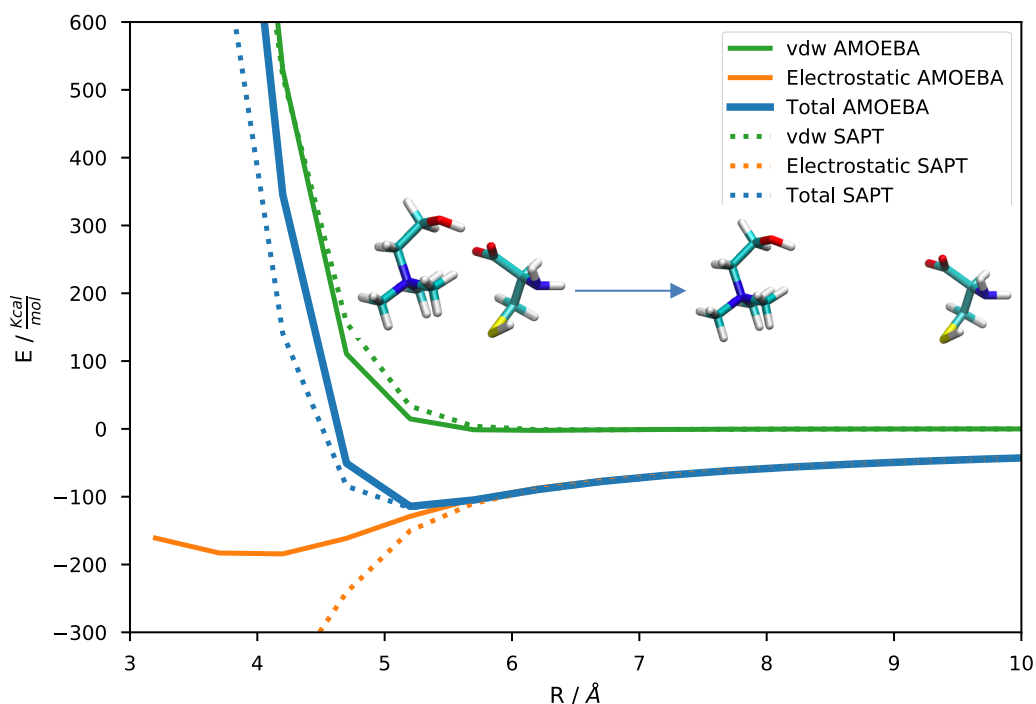


Figure 2: Detailed analysis of the interaction energies in a single ionic couple of [Ch][Cys]. We compare the total interaction energy (blue), the electrostatic contribution (orange) and the Van der Waals one (green) from the FF (solid lines) and from SAPT (dotted lines).

3.2 Bulk simulations

All of the 9 liquids stemming from the AA anions have been simulated in their bulk phase under xyz periodic boundary conditions using Tinker-HP [68]. The typical simulation included 100 ionic couples in a periodic arrangement of cubic cells. Initially an NPT

ensemble at 1 atm and room temperature for 1-2 ns was used to equilibrate the liquids up to a stable density. Subsequently, for [Ala], [Cys], [His], [Asp], [Val] and [Phe] we have continued the simulation with NVT to compute additional structural indicators and the cohesive energy density (see Table S2). The times of the NVT portion of the simulation is around 2 ns that is largely sufficient to collect structural data. Only for [Cys], we have carried out 20 ns of NVT simulation. In all cases, a further increase of the production time did not significantly modify the shape of the results presented here.

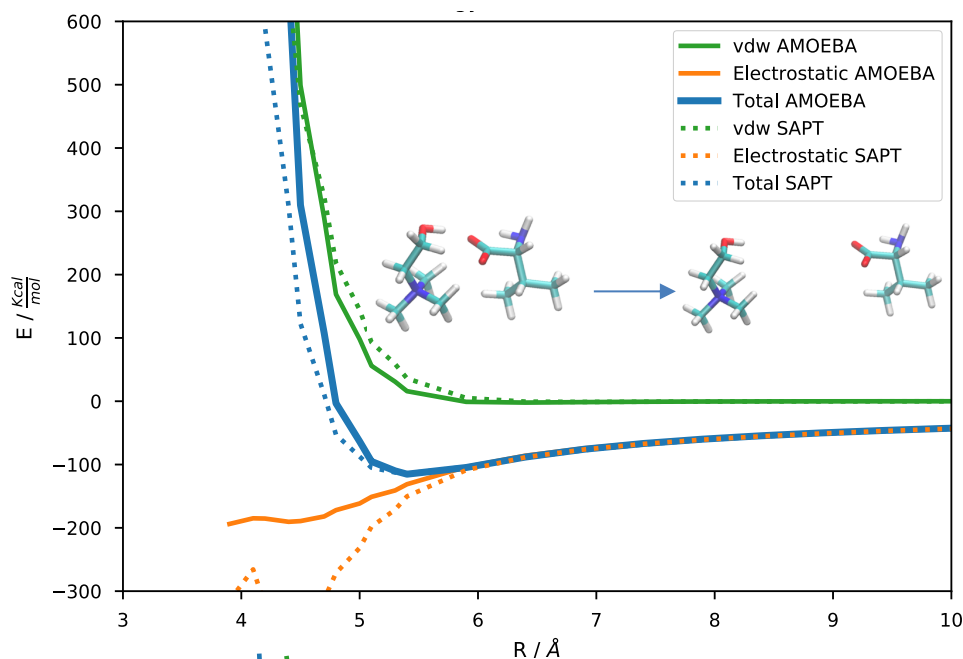


Figure 3: Detailed analysis of the interaction energies in a single ionic couple of [Ch][Val]. We compare the total interaction energy (blue), the electrostatic contribution (orange) and the Van der Waals one (green) from the FF (solid lines) and from SAPT (dotted lines).

The NPT simulations produced converged densities that can be compared with experimental literature data [69,70]. For [Ala], [Ser], [Cys], [Gly], [Phe], [His], [Lys] and [Asp] we have obtained, respectively 1.07, 1.17, 1.17, 1.12, 1.11, 1.17, 1.08 and 1.21 g cm^{-3} . All these values slightly underestimate the experimental density by few percent, with a maximum deviation of -3.8% in the case of [Ch][Ala] (see Table S2). The negative

error on the density is very likely due to the slight overestimation of the repulsive term at short range of our FF model.

In order to further validate the bulk properties produced by the FF we present few selected geometrical indicators that we compare with the analogous data from the simulations reported previously by us in refs. [37,38] which were performed with Born-Oppenheimer (ab-initio) molecular dynamics (AIMD). Those simulations were shown to reproduce to a very good extent the experimental bulk structure as obtained by experimental X-ray diffraction structure factors and can be considered quite accurate, especially in determining the short-range structure of the fluid. This is, in our opinion, a stringent test of the ability of present FF to provide an accurate picture of the local ordering of the bulk phase. We limit the discussion to the [Ala] and [Cys] anions, chosen as representative ones, while analogous, exemplar data on [Val], [Phe], [His] and [Asp] are reported in the SI in Section S4.

In Figure 4 we report a set of different radial distribution functions ($g(r)$) for the relevant anion-cation interaction for [Ch][Ala] as collected over the NVT portion of the simulation. Apart from the slight noise in the AIMD results (due to its short propagation times of only ~ 60 ps) the two sets of data are in excellent agreement. The distances involved in the anion-cation hydrogen bond (green line in Figure 4) is perfectly reproduced, as well as the average distance between the centers of mass of the two oppositely charged molecular ions (blue line in Figure 4). A more stringent test of the FF is provided in Figure 5, where we report the radial distributions of the anion-anion and cation-cation interactions which are typically weaker and less structured (being in a second solvation shell) than the cation-anion previously illustrated. On the left in Figure 5 we can see how the distance distribution of the centers of mass of two nearest cations (blue lines) is reproduced correctly by our FF with respect to the ab-initio calculations.

Remarkably, also the second peak in the radial distribution at 10-11 Å is correctly localized. The distribution of distances between the cation central nitrogen and the –OH of another cation (green lines) is also correctly reproduced, albeit its second peak is slightly shifted at a larger distance with respect to AIMD. The anion-anion interactions are an important, but elusive feature of these ILs [71]. For [Ala], these interactions should be almost negligible, and pertain mainly to weak hydrogen bonded interactions between the –NH₂ and the –COO[–] groups (Figure 5 on the right, green line). It can be clearly seen as this interaction is properly modelled by the present FF, although slightly overestimated with respect to AIMD.

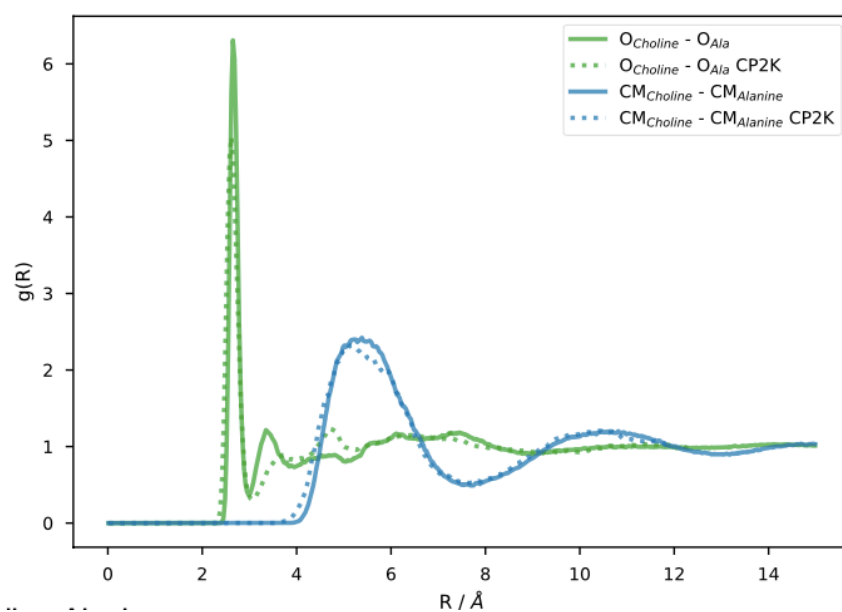


Figure 4: Anion-Cation radial distribution functions for [Ch][Ala]: the solid lines are from the present Amoeba FF; the dotted lines from CP2K, DFT-based MD. Green lines, COO—OH distance; blue lines, centers of mass distance of the two molecular ions.

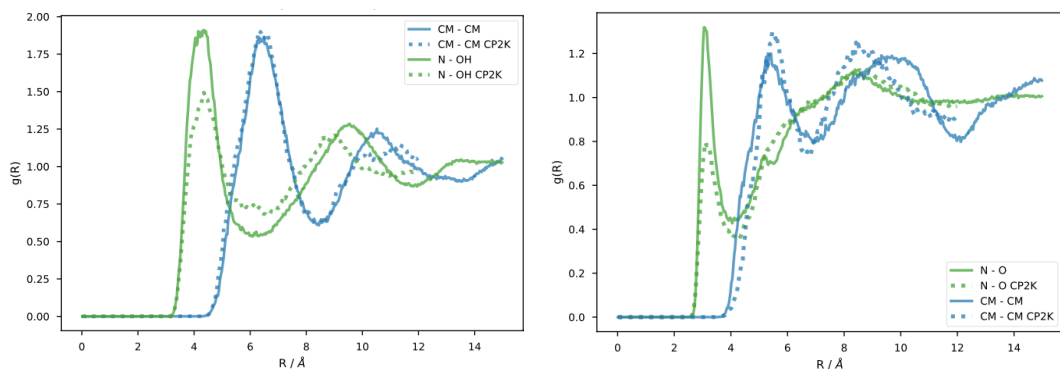


Figure 5: Radial distribution functions for [Ch][Ala]. Solid lines present Amoeba FF; dotted lines CP2K DFT-based MD. Left: cation-cation distances between the centers of mass (blue) and between the ammonium N and the OH of another cation. Right: anion-anion intermolecular distances between the centers of mass (blue) and between COO and NH₂ (green).

The comparison between the bulk X-ray static structure factor as computed from the present simulations and those performed with CP2K (which we have already shown to compare well with experimental data in refs. [37,62]) is reported in Figure 6 on the left. The structure factors reported here have been obtained using the equations reported in ref. [72] and the Travis code [73]. It is evident how our FF reproduce almost perfectly the short-range structure of the fluid phase.

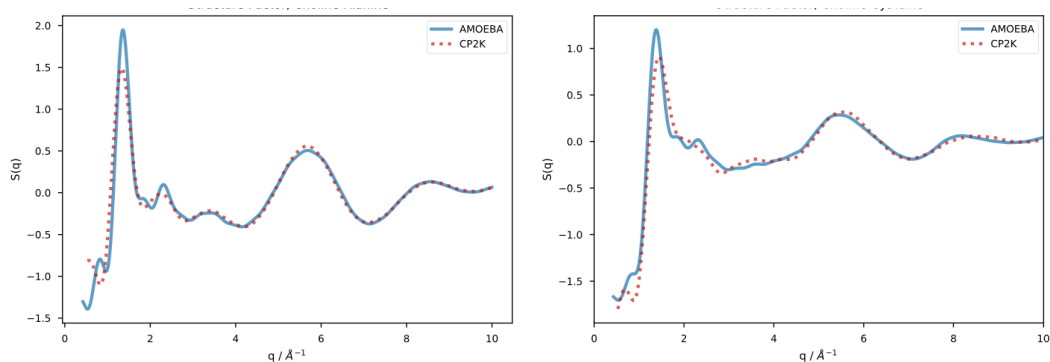


Figure 6: Static X-ray structure factors for [Ch][Ala] (left) and [Ch][Cys] (right): the solid lines are from the present Amoeba FF; the dotted lines from CP2K, DFT-based MD. Due to limitations in cell sizes, the data below 1 Å⁻¹ are unreliable.

An analogous set of $g(r)$ is reported in Figures 7 and 8 for the [Ch][Cys] liquid. Figure 7 demonstrates how the FF is able to reproduce the correct distances of the O—O hydrogen bond between the cation and the anion (green line). There are few slight differences

though between the CP2K data and the present FF: the presence of shoulder at 2.5 Å in the Amoeba data shows that the hydrogen bond between the cation –OH and the carboxylate is less symmetric than in the CP2K simulations, but it could be also due to a better sampling of the molecular motions around the bond due to the longer production time of the FF simulation. The average relative position between the cation and anion centers of mass is substantially the same (blue line).

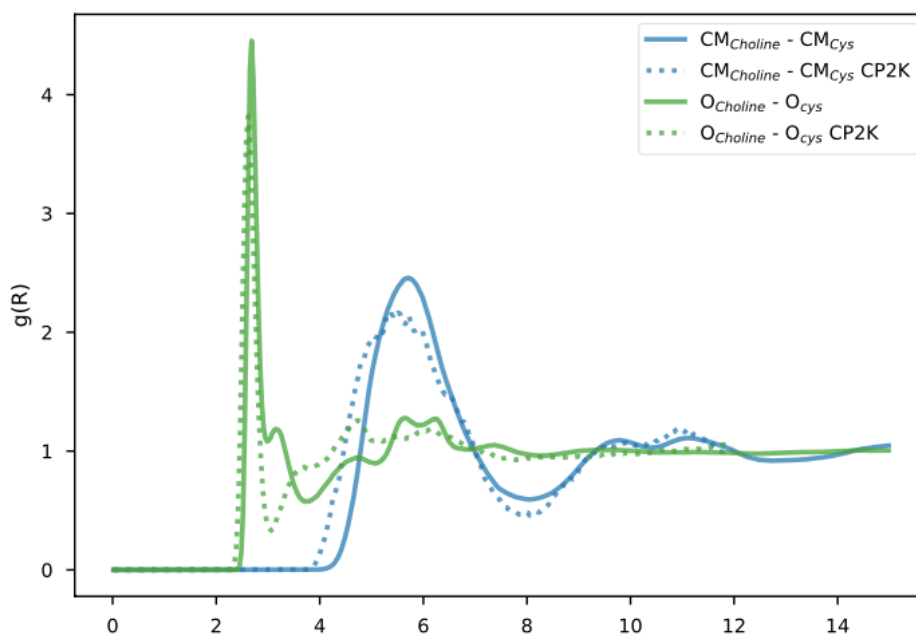


Figure 7: Anion-Cation radial distribution functions for [Ch][Cys]: the solid lines are from the present Amoeba FF; the dotted lines from CP2K, DFT-based MD. Green lines, COO—OH distance; blue lines, centers of mass distance of the two molecular ions.

In Figure 8 we report the anion-anion radial distributions for [Ch][Cys]. Since this is an important interaction for possibly acidic AA such as Cys because it could give rise to isomerization reaction (see our work in ref. [36]), we have consistently checked that the FF was able to account for inter-anionic aggregation phenomena. The position of the inter-anionic hydrogen bond is well reproduced with respect to the ab-initio data, albeit the intensity of the interaction is slightly overestimated by our model. For the same reason the relative positions of two anions (blue line) is more short-ranged (of about 1 Å) with

respect to the CP2K data, but this, again, could be due to the better statistics of our simulations due to the short running time of the CP2K ones. The comparison of the X-ray structure factors from Amoeba and from CP2K is presented in Figure 6 on the right for [Ch][Cys].

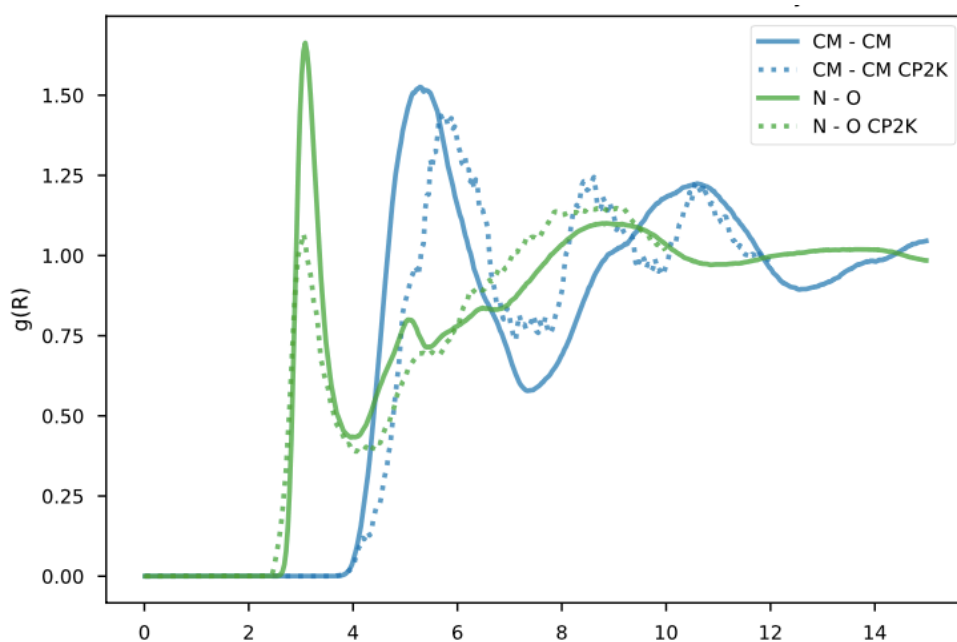


Figure 8: Anion-Anion radial distribution functions for [Ch][Cys]: the solid lines are from the present Amoeba FF; the dotted lines from CP2K, DFT-based MD. Green lines, COO—NH₂ distance; blue lines, centers of mass distance of the two molecular ions.

4. Conclusions

We have presented an extension of the Amoeba force field to biocompatible ionic liquids based on AA anions and choline. The FF has been derived from ab-initio calculations on the isolated molecular ions. It has been built trying to be as transferable and as compatible as possible with the existing Amoeba parametrization, hence without peculiar adjustments (short-range repulsion or charge scaling, for example). The FF performance in reproducing the interaction energies of the simplest aggregates (ionic couples, and small clusters) has been validated by direct comparison with ab-initio DFT predictions

and yielded a good agreement where the FF is able to reproduce the overall interaction within less than 10% difference with respect to the ab-initio data. The energy decomposition along the dissociating paths of single ionic couples further proved that the new parametrization is able to reproduce both the van der Waals and the electrostatic contribution to the interaction energy with great accuracy.

The bulk properties of the fluid are more difficult to test extensively since for many of these ionic liquids there is a lack of thermodynamic experimental measurements. The FF is reproducing the experimental densities with an error well within 3% for most of them. The short range structure of the bulk fluid provided by the new parametrization has been extensively tested against analogous, pre-existing AIMD simulations employing DFT. Again, the FF clearly showed the ability to reproduce the bulk fluid structure with results that are invariably consistent with the ab-initio data, including the X-ray static structure factors.

Acknowledgements

This work received financial support from “La Sapienza” (grants n. RG120172B4099747, RM11916B658EF0BA). All authors gratefully acknowledge the computational support of CINECA (grants IsC78_LLL-2 and IsC69_LLL).

Bibliography

- [1] Gontrani L. Choline-amino acid ionic liquids: past and recent achievements about the structure and properties of these really “green” chemicals. *Biophys Rev.* 2018;10:873–880.
- [2] Gomes JM, Silva SS, Reis RL. Biocompatible ionic liquids: fundamental behaviours and applications. *Chem Soc Rev.* 2019;48:4317–4335.
- [3] Fedotova MV, Kruchinin SE, Chuev GN. Features of local ordering of biocompatible ionic liquids: The case of choline-based amino acid ionic liquids. *J Mol Liq.* 2019;296:112081.

- [4] Moshikur R, Chowdhury R, Moniruzzaman M, et al. Biocompatible ionic liquids and their applications in pharmaceuticals. *Green Chem.* 2020;22:8116–8139.
- [5] Dhattarwal HS, Kashyap HK. Unique and generic structural features of cholinium amino acid-based biocompatible ionic liquids. *Phys Chem Chem Phys.* 2021;23:10662–10669.
- [6] Le Donne A, Bodo E. Cholinium amino acid-based ionic liquids. *Biophys Rev* [Internet]. 2021 [cited 2021 Jan 14]; Available from: <http://link.springer.com/10.1007/s12551-021-00782-0>.
- [7] Zubeltzu J, Formoso E, Rezabal E. Lignin solvation by ionic liquids: The role of cation. *J Mol Liq.* 2020;303:112588.
- [8] Stettner T, Balducci A. Protic ionic liquids in energy storage devices: past, present and future perspective. *Energy Storage Mater.* 2021;40:402–414.
- [9] Jónsson E. Ionic liquids as electrolytes for energy storage applications – A modelling perspective. *Energy Storage Mater.* 2020;25:827–835.
- [10] Kobzar YL, Fatyeyeva K. Ionic liquids as green and sustainable steel corrosion inhibitors: Recent developments. *Chem Eng J.* 2021;425:131480.
- [11] Xu P, Liang S, Zong M-H, et al. Ionic liquids for regulating biocatalytic process: Achievements and perspectives. *Biotechnol Adv.* 2021;51:107702.
- [12] Krishnan A, Gopinath KP, Vo D-VN, et al. Ionic liquids, deep eutectic solvents and liquid polymers as green solvents in carbon capture technologies: a review. *Environ Chem Lett.* 2020;18:2031–2054.
- [13] Paucar NE, Kiggins P, Blad B, et al. Ionic liquids for the removal of sulfur and nitrogen compounds in fuels: a review. *Environ Chem Lett.* 2021;19:1205–1228.
- [14] Liu F, Yu J, Qazi AB, et al. Metal-Based Ionic Liquids in Oxidative Desulfurization: A Critical Review. *Environ Sci Technol.* 2021;55:1419–1435.
- [15] Shaikh AR, Ashraf M, AlMayef T, et al. Amino acid ionic liquids as potential candidates for CO₂ capture: Combined density functional theory and molecular dynamics simulations. *Chem Phys Lett.* 2020;745:137239.
- [16] Alizadeh V, Esser L, Kirchner B. How is CO₂ absorbed into a deep eutectic solvent? *J Chem Phys.* 2021;154:094503.
- [17] Wang L, Zhang Y, Liu Y, et al. SO₂ absorption in pure ionic liquids: Solubility and functionalization. *J Hazard Mater.* 2020;392:122504.
- [18] Cho C-W, Pham TPT, Zhao Y, et al. Review of the toxic effects of ionic liquids. *Sci Total Environ.* 2021;786:147309.
- [19] Chen Y, Mu T. Revisiting greenness of ionic liquids and deep eutectic solvents. *Green Chem Eng.* 2021;2:174–186.

- [20] Magina S, Barros-Timmons A, Ventura SPM, et al. Evaluating the hazardous impact of ionic liquids – Challenges and opportunities. *J Hazard Mater.* 2021;412:125215.
- [21] Kumari P, Pillai VVS, Benedetto A. Mechanisms of action of ionic liquids on living cells: the state of the art. *Biophys Rev.* 2020;12:1187–1215.
- [22] Benedetto A. Room-temperature ionic liquids meet bio-membranes: the state-of-the-art. *Biophys Rev.* 2017;9:309–320.
- [23] Benedetto A, Ballone P. Room Temperature Ionic Liquids Meet Biomolecules: A Microscopic View of Structure and Dynamics. *ACS Sustain Chem Eng.* 2016;4:392–412.
- [24] Zandu SK, Chopra H, Singh I. Ionic Liquids for Therapeutic and Drug Delivery Applications. *Curr Drug Res Rev.* 2020;12:26–41.
- [25] Saptal VB, Bhanage BM. Bifunctional Ionic Liquids Derived from Biorenewable Sources as Sustainable Catalysts for Fixation of Carbon Dioxide. *ChemSusChem.* 2017;10:1145–1151.
- [26] Baaqel H, Díaz I, Tulus V, et al. Role of life-cycle externalities in the valuation of protic ionic liquids – a case study in biomass pretreatment solvents. *Green Chem.* 2020;22:3132–3140.
- [27] Asim AM, Uroos M, Muhammad N. Extraction of lignin and quantitative sugar release from biomass using efficient and cost-effective pyridinium protic ionic liquids. *RSC Adv.* 2020;10:44003–44014.
- [28] Stettner T, Lingua G, Falco M, et al. Protic Ionic Liquids-Based Crosslinked Polymer Electrolytes: A New Class of Solid Electrolytes for Energy Storage Devices. *Energy Technol.* 2020;8:2000742.
- [29] Gerlach P, Burges R, Lex-Balducci A, et al. Aprotic and Protic Ionic Liquids as Electrolytes for Organic Radical Polymers. *J Electrochem Soc.* 2020;167:120546.
- [30] Sivapragasam M, Moniruzzaman M, Goto M. An Overview on the Toxicological Properties of Ionic Liquids toward Microorganisms. *Biotechnol J.* 2020;15:1900073.
- [31] Bui-Le L, Clarke CJ, Bröhl A, et al. Revealing the complexity of ionic liquid–protein interactions through a multi-technique investigation. *Commun Chem.* 2020;3:55.
- [32] Wakayama R, Uchiyama S, Hall D. Ionic liquids and protein folding—old tricks for new solvents. *Biophys Rev.* 2019;11:209–225.
- [33] Lim GS, Klähn M. On the Stability of Proteins Solvated in Imidazolium-Based Ionic Liquids Studied with Replica Exchange Molecular Dynamics. *J Phys Chem B.* 2018;122:9274–9288.

- [34] Kirchner B. Ionic Liquids from Theoretical Investigations. In: Kirchner B, editor. *Ion Liq* [Internet]. Berlin, Heidelberg: Springer Berlin Heidelberg; 2008 [cited 2022 Mar 4]. p. 213–262. Available from: http://link.springer.com/10.1007/128_2008_36.
- [35] Amith WD, Araque JC, Margulis CJ. A Pictorial View of Viscosity in Ionic Liquids and the Link to Nanostructural Heterogeneity. *J Phys Chem Lett.* 2020;11:2062–2066.
- [36] Adenusi H, Le Donne A, Porcelli F, et al. Ab Initio Molecular Dynamics Study of Phospho-Amino Acid-Based Ionic Liquids: Formation of Zwitterionic Anions in the Presence of Acidic Side Chains. *J Phys Chem B.* 2020;124:1955–1964.
- [37] Campetella M, Bodo E, Montagna M, et al. Theoretical study of ionic liquids based on the cholinium cation. *Ab initio* simulations of their condensed phases. *J Chem Phys.* 2016;144:104504.
- [38] Campetella M, Bodo E, Caminiti R, et al. Interaction and dynamics of ionic liquids based on choline and amino acid anions. *J Chem Phys.* 2015;142:234502.
- [39] Kirchhecker S, Esposito D. Amino acid based ionic liquids: A green and sustainable perspective. *Curr Opin Green Sustain Chem.* 2016;2:28–33.
- [40] Yan T, Burnham CJ, Del Pópolo MG, et al. Molecular Dynamics Simulation of Ionic Liquids: The Effect of Electronic Polarizability. *J Phys Chem B.* 2004;108:11877–11881.
- [41] Schröder C. Comparing reduced partial charge models with polarizable simulations of ionic liquids. *Phys Chem Chem Phys.* 2012;14:3089.
- [42] Bedrov D, Piquemal J-P, Borodin O, et al. Molecular Dynamics Simulations of Ionic Liquids and Electrolytes Using Polarizable Force Fields. *Chem Rev.* 2019;119:7940–7995.
- [43] Tu Y-J, Lin Z, Allen MJ, et al. Molecular dynamics investigation of water-exchange reactions on lanthanide ions in water/1-ethyl-3-methylimidazolium trifluoromethylsulfate ([EMIm][OTf]). *J Chem Phys.* 2018;148:024503.
- [44] Philippi F, Goloviznina K, Gong Z, et al. Charge transfer and polarisability in ionic liquids: a case study. *Phys Chem Chem Phys.* 2022;24:3144–3162.
- [45] Szabadi A, Elfgén R, Macchieraldo R, et al. Comparison between ab initio and polarizable molecular dynamics simulations of 1-butyl-3-methylimidazolium tetrafluoroborate and chloride in water. *J Mol Liq.* 2021;337:116521.
- [46] Bodo E. Perspectives in the Computational Modeling of New Generation, Biocompatible Ionic Liquids. *J Phys Chem B.* 2022;126:3–13.
- [47] McDaniel JG, Yethiraj A. Understanding the Properties of Ionic Liquids: Electrostatics, Structure Factors, and Their Sum Rules. *J Phys Chem B.* 2019;123:3499–3512.

- [48] Vázquez-Montelongo EA, Vázquez-Cervantes JE, Cisneros GA. Current Status of AMOEBA-IL: A Multipolar/Polarizable Force Field for Ionic Liquids. *Int J Mol Sci.* 2020;21:697.
- [49] Goloviznina K, Canongia Lopes JN, Costa Gomes M, et al. Transferable, Polarizable Force Field for Ionic Liquids. *J Chem Theory Comput.* 2019;15:5858–5871.
- [50] Dommert F, Wendler K, Berger R, et al. Force Fields for Studying the Structure and Dynamics of Ionic Liquids: A Critical Review of Recent Developments. *ChemPhysChem.* 2012;13:1625–1637.
- [51] Schröder C. Proteins in Ionic Liquids: Current Status of Experiments and Simulations. *Top Curr Chem.* 2017;375:25.
- [52] Goloviznina K, Gong Z, Padua AAH. The CL&Pol polarizable force field for the simulation of ionic liquids and eutectic solvents. *WIREs Comput Mol Sci* [Internet]. 2021 [cited 2021 Oct 6]; Available from: <https://onlinelibrary.wiley.com/doi/10.1002/wcms.1572>.
- [53] Goloviznina K, Gong Z, Costa Gomes MF, et al. Extension of the CL&Pol Polarizable Force Field to Electrolytes, Protic Ionic Liquids, and Deep Eutectic Solvents. *J Chem Theory Comput.* 2021;17:1606–1617.
- [54] Jaffrelot Inizan T, Célerse F, Adjoua O, et al. High-resolution mining of the SARS-CoV-2 main protease conformational space: supercomputer-driven unsupervised adaptive sampling. *Chem Sci.* 2021;12:4889–4907.
- [55] Ponder JW, Wu C, Ren P, et al. Current Status of the AMOEBA Polarizable Force Field. *J Phys Chem B.* 2010;114:2549–2564.
- [56] Zhang C, Lu C, Jing Z, et al. AMOEBA Polarizable Atomic Multipole Force Field for Nucleic Acids. *J Chem Theory Comput.* 2018;14:2084–2108.
- [57] Burnham CJ, Li J, Xantheas SS, et al. The parametrization of a Thole-type all-atom polarizable water model from first principles and its application to the study of water clusters ($n = 2-21$) and the phonon spectrum of ice Ih. *J Chem Phys.* 1999;110:4566–4581.
- [58] Wu JC, Chattree G, Ren P. Automation of AMOEBA polarizable force field parameterization for small molecules. *Theor Chem Acc.* 2012;131:1138.
- [59] Seeger ZL, Izgorodina EI. A Systematic Study of DFT Performance for Geometry Optimizations of Ionic Liquid Clusters. *J Chem Theory Comput.* 2020;16:6735–6753.
- [60] Rackers JA, Wang Z, Lu C, et al. Tinker 8: Software Tools for Molecular Design. *J Chem Theory Comput.* 2018;14:5273–5289.
- [61] Hollóczki O, Malberg F, Welton T, et al. On the origin of ionicity in ionic liquids. Ion pairing versus charge transfer. *Phys Chem Chem Phys.* 2014;16:16880–16890.

- [62] Campetella M, Montagna M, Gontrani L, et al. Unexpected proton mobility in the bulk phase of cholinium-based ionic liquids: new insights from theoretical calculations. *Phys Chem Chem Phys*. 2017;19:11869–11880.
- [63] Lin Y-S, Li G-D, Mao S-P, et al. Long-Range Corrected Hybrid Density Functionals with Improved Dispersion Corrections. *J Chem Theory Comput*. 2013;9:263–272.
- [64] Shil S, Herrmann C. Performance of range-separated hybrid exchange-correlation functionals for the calculation of magnetic exchange coupling constants of organic diradicals. *J Comput Chem*. 2018;39:780–787.
- [65] Benedetto A, Bodo E, Gontrani L, et al. Amino Acid Anions in Organic Ionic Compounds. An *ab Initio* Study of Selected Ion Pairs. *J Phys Chem B*. 2014;118:2471–2486.
- [66] Jeziorski B, Moszynski R, Szalewicz K. Perturbation Theory Approach to Intermolecular Potential Energy Surfaces of van der Waals Complexes. *Chem Rev*. 1994;94:1887–1930.
- [67] Turney JM, Simmonett AC, Parrish RM, et al. Psi4: an open-source *ab initio* electronic structure program: Psi4: an electronic structure program. *Wiley Interdiscip Rev Comput Mol Sci*. 2012;2:556–565.
- [68] Jolly L-H, Duran A, Lagardère L, et al. Raising the Performance of the Tinker-HP Molecular Modeling Package [Article v1.0]. *Living J Comput Mol Sci* [Internet]. 2019 [cited 2022 Feb 25];1. Available from: <https://www.livecomsjournal.org/article/10409-raising-the-performance-of-the-tinker-hp-molecular-modeling-package-article-v1-0>.
- [69] Tao D-J, Cheng Z, Chen F-F, et al. Synthesis and Thermophysical Properties of Biocompatible Cholinium-Based Amino Acid Ionic Liquids. *J Chem Eng Data*. 2013;58:1542–1548.
- [70] De Santis S, Masci G, Casciotta F, et al. Cholinium-amino acid based ionic liquids: a new method of synthesis and physico-chemical characterization. *Phys Chem Chem Phys*. 2015;17:20687–20698.
- [71] Le Donne A, Adenusi H, Porcelli F, et al. Hydrogen Bonding as a Clustering Agent in Protic Ionic Liquids: Like-Charge vs Opposite-Charge Dimer Formation. *ACS Omega*. 2018;3:10589–10600.
- [72] Hollóczki O, Macchiagodena M, Weber H, et al. Triphilic Ionic-Liquid Mixtures: Fluorinated and Non-fluorinated Aprotic Ionic-Liquid Mixtures. *ChemPhysChem*. 2015;16:3325–3333.
- [73] Brehm M, Thomas M, Gehrke S, et al. TRAVIS—A free analyzer for trajectories from molecular simulation. *J Chem Phys*. 2020;152:164105.